Fe^{3+} as the Main form of Iron Ions in Iron-Lead-Phosphate Glasses

Sh. N. Radwan

Physics Department Faculty of Science (Girls), Al-Azhar University, Nasr City, Cairo, Egypt.

Electron Paramagnetic Resonance EPR, hydrostatic density (ρ), molar volume (V), differential thermal analysis (DTA) and infrared spectroscopy measurements have been employed to investigate the effect of Fe_2O_3 content on the physical properties of a series of iron-lead-phosphate glasses in the system (100-2x)Fe_2O_3–xPbO-xP_2O_5 with x = 12.5, 15, 17.5 and 20 mol%. The samples have been prepared by melting the mixtures under normal atmosphere at 1300 ± 20° C. The EPR spectra, for all samples, reveal the presence of an intensive resonance peak at g ~ 2 which is attributed to Fe^{3+} ion located in a site with high symmetry. A monotonic increase in (ρ) value and a corresponding decrease of the (V) value are also detected with increasing Fe_2O_3. The increasing value of the glass transition temperature Tg with Fe_2O_3 content as detected by DTA indicates the increase of the degree of bridging. The increased (T_c-T_g) value reveals the stability of iron-rich phosphate glasses. The experimental IR absorption bands have been identified. The data have been discussed in terms of the formation of Fe^{3+} as the main form of iron ions in iron-lead-phosphate glasses.

1. Introduction:

Electron paramagnetic resonance spectroscopy is a powerful experimental technique which can be used to get information about the structural and dynamic phenomena of materials. EPR studies of glasses containing transition metal ions (TMI) have been used to obtain information regarding the glassy network and to identify the site symmetry around the TMI. Several studies have been made on the EPR spectra of TMI in oxide glasses [1-6]. Sales and Boatner [7] found that iron-lead-phosphate glasses were more durable than many borosilicate glasses and they suggested the use of these glasses for vitrifying nuclear waste. Shih as well as others [8-13] suggested that the addition of one or more of SnO, PbO, ZnO, Al_2O_3 and Fe_2O_3 oxides to phosphate glasses resulted in the formation of Sn-O-P, Pb-O-P, Zn-O-P, Al-O-P and Fe-O-P bonds, which lead to an improvement in the chemical durability of the modified phosphate glasses. Of all additions to phosphate glasses, PbO is the only one which reduces the dissolution rate and softening temperature at the same time [14-16]. On the other hand, the structural role of PbO in many oxide glasses is unique since PbO is known to play a dual structural role, both as a network modifier [17], and as a network former [18]. The objective of the present work is to report the effect of the Fe_2O_3 content on the physical properties of a series of iron rich glasses containing equimolar ratio of PbO and P_2O_5.

2. Experimental:

The glass samples were prepared by mixing the appropriate amounts of analar grade chemicals Fe_2O_3, PbO, P_2O_5 in the ratio (100-2x) Fe_2O_3–x PbO–xP_2O_5 (x=12.5, 15, 17.5 and 20 mol %). The mixture was melted in a silica crucible at normal atmosphere at 1300 ± 20°C for 3 hours. The melt was cast in iron preheated moulds on iron plate, and was immediately transferred to an annealing furnace held at 250°C for 15 minutes. Gradual self cooling to room temperature was then achieved. Part of the prepared samples was grinded into fine powder and sieved using 200 mesh sieve to be used for different purposes. The amorphous state of the prepared samples was checked by x-ray diffraction. Electron paramagnetic resonance spectra were made at room temperature using a Varian X- band spectrometer with a modulation frequency of 100 KHz. The infrared spectra were recorded over the range 200-2000 cm^{-1} at room temperature using FTIR spectrometer (Beckman 4220). Differential thermal analysis was carried out from room temperature up to 750°C with heating rate of 10°C/min using Perkin Elmer DTA apparatus. The density measurement of the samples was determined experimentally using xylene as the buoyancy liquid, while the theoretical density was calculated according to the relation:

$$\rho_{th} = 1 / \Sigma (a_i / \rho_i) \qquad (1)$$

where a_i is the weight fraction of the i $^{\underline{th}}$ oxide and ρ_i is the density of the i $^{\underline{th}}$ oxide.

The molar volume was calculated from the experimentally determined density (ρ) according to the relation:

$$V = \Sigma (M_i N_i) / \rho \qquad (2)$$

where M_i and N_i are the molecular weight and the mole fraction of the different constituent oxides respectively.

3. Results and discussion:

3.1. Electron paramagnetic resonance:

The EPR spectrum may be interpreted by the spin Hamilitonian

$$H = B\ g\ H\ S + I\ A\ S \qquad (3)$$

where B is the Bohr magneton, g is the spectroscopy splitting factor, A is the hyperfine structure tensor, and H, I, S are the static magnetic field operator, the electron spin operator and the nuclear spin operator respectively. Fig.(1) is a typical EPR spectra for the samples under study measured at room temperature. As shown in the figure, an intense resonance peak at g ~ 2 is a characteristic feature for all the EPR recorded spectra. Absence of the resonance at g ~ 4.3 and g ~ 6 is noticed except for the sample with 60 mol % Fe_2O_3 which shows a weak resonance peak at g ~ 4.3. This may be due to the high concentration of iron included in the prepared samples. As the resonance from Fe^{2+} ion is undetectable at room temperature [19,20], one may suggest that the present observed resonance peaks are due to Fe^{3+} ions. On the other hand, the high intensity of the g ~ 2 resonance indicates that almost all the incorporated iron form clusters.

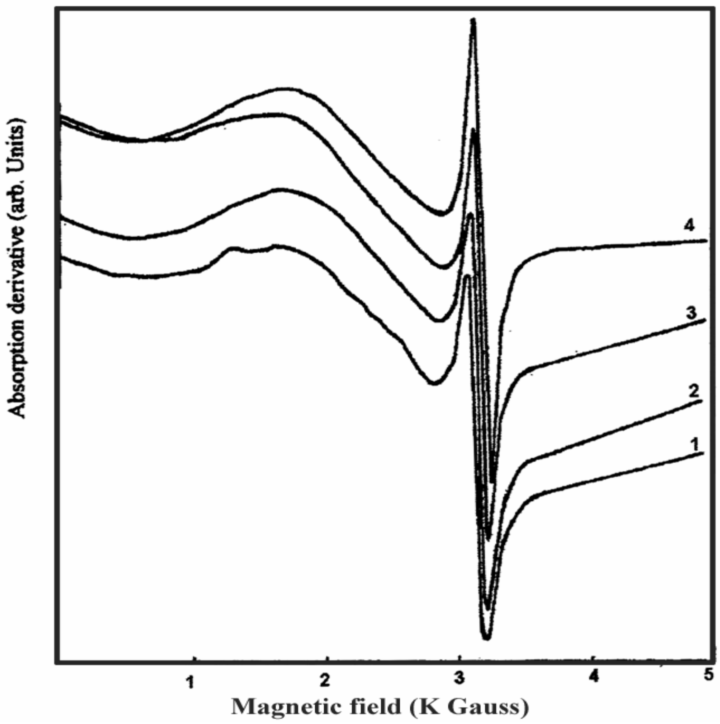

Fig.(1): EPR spectra of (100- 2x) Fe_2O_3 – x PbO – x P_2O_5 glasses Numbers in the figure represent glass numbers in table (1).

The features of the EPR spectra can be qualitatively explained as follows [21- 23] : the large resonance peak for Fe^{3+} at $g \sim 2$ can only occur if the Fe^{3+} is located in a site where the crystal field interaction energy is less than the magnetic Zeeman energy. This case would correspond to iron located in a site with a higher symmetry. On the other hand, the resonance at $g \sim 4.3$ is due to an environment, where the interaction energy between the surrounding crystal field and the Fe^{3+} ion is larger than the Zeeman energy. This case would correspond to iron in a relatively low symmetry site in the glass structure. Fig.(1) clearly shows that with increasing iron content, the weak resonance at $g \sim 4.3$ is rapidly broadened out; presumably due to spin – spin interactions between neighboring iron ions. The $g \sim 2$ resonance peak is, on the contrary, not sensitive to this effect as its width becomes narrower with increasing the iron content. In fact, this peak is known to appear when the iron content is sufficiently large for the iron–iron distance to be small enough for the spin–spin interaction to be effective[24] .

The integrated area is determined by the concentration of paramagnetic ions present in each glass. The area under the resonance peaks have been calculated using the approximation $A = W\ I\ (\Delta\ H)^2$ where W is a weighting factor necessary for suitable correction for the weight of the sample, I is the relative peak to peak intensity and Δ H is the line width in derivative plots. Table 1 and Fig.(2) represent the calculated areas as a function of Fe_2O_3 content. It is clear that, the area decreases rapidly as the PbO content increases in replacement of Fe_2O_3. This result can be explained as follows: Addition of PbO gives rise to the formation of non bridging oxygen attached to Fe^{3+} ions.

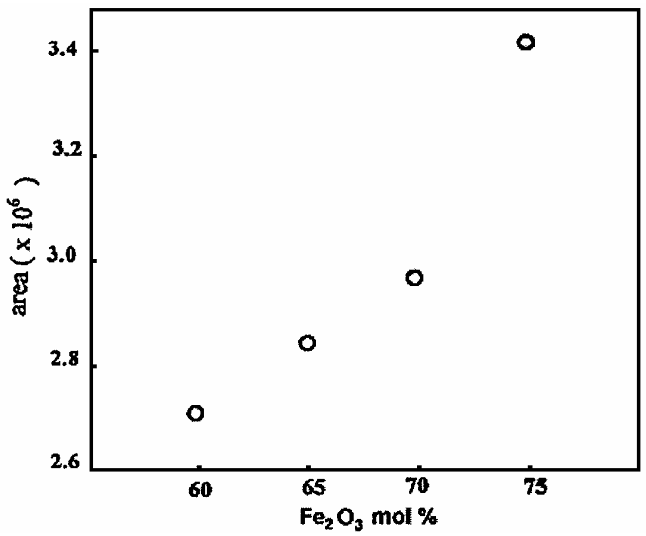

Fig.(2): Variation of area under the peak with iron content (mole %) in (100- 2x) Fe_2O_3 – x PbO – x P_2O_5 glasses .

As a result the iron-iron distance increases due to the fact that now two non–bridging oxygen have to be accommodated instead of the bridging one which was present earlier [25]. This weaknesses the spin-spin interactions and hence decreases the area of the g ~ 2 resonance. If the formed non-bridging oxygen are attached to phosphorus ions, the iron-iron distance will not appreciably affected. It is therefore obvious that, the area under the peak is more likely to be controlled by the PbO content.

3.2. Hydrostatic density, molar volume and thermal analysis:

The variation of both the experimental and theoretical data of the hydrostatic density with iron content is given in Fig. (3). The figure shows a monotonic change in density with iron content. Such monotonic behavior indicates that the structure of the glass does not change with composition. In fact, a change in the structure would be reflected by a sharp change in the slope of the plot of density against composition[26]. The calculated density deviation (ρ_{th} - ρ_{exp}) is found to be always positive and increases with increasing Fe_2O_3 content for all the compositions under study. This is in agreement with the role of Pb^{2+} in crosslinking the polymeric chains.

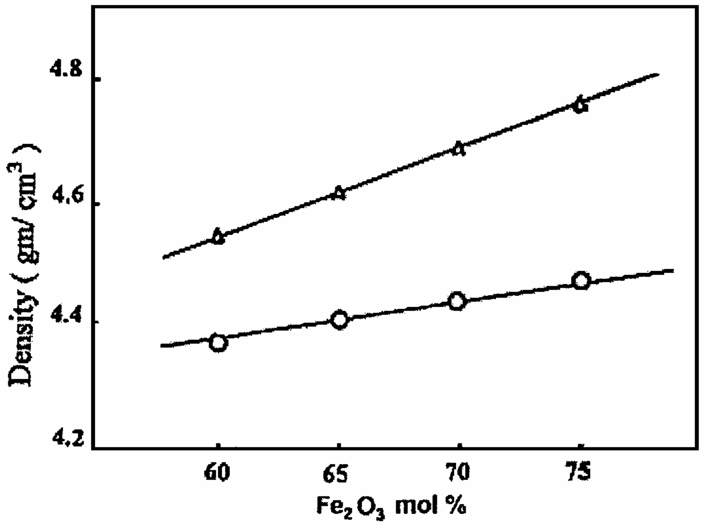

Fig.(3): Variation of density with iron content (mole %) in (100- 2x) Fe_2O_3 – xPbO – x P_2O_5 glasses . O experimental data Δ theoretical data

The molar volume (V) of the compositions under study is calculated according to Eqn. (2) and illustrated in Table 1. A decrease in the value of V is detected as increasing the Fe_2O_3 content. This decrease may be a result of a decreasing of the Fe^{3+} - Fe^{3+} distance, thereby enhancing the formation of clusters. This agrees well with the increased area of the g ~2 resonance line as shown in Table (1).

Figure.(4) displays the experimental DTA thermograms of the compositions under study. The glass transition temperatures (T_g) as well as the crystallization temperatures (T_c) deduced from the thermograms are given in Table (1). We notice that the values of both T_g and T_c continuously shift to higher temperatures with increasing iron content. It is well known that T_g value is closely correlated to the change in the coordination number of the glass forming atoms (network former) and with the formation of non-bridging oxygen, which correspond to the depolymerization of the glass skeleton [27]. In general, it is known that T_g increases with increasing the degree of bridging and contrary to this, the formation of non-bridging oxygen decreases it Therefore, one can conclude that the increase detected in T_g value from 551 to 564°C (Table (1)) can be ascribed to a corresponding increase in the degree of bridging with increasing Fe_2O_3 content. It is to be also noted that the increased ($T_c - T_g$) difference value for the higher Fe_2O_3 sample reveals the stability of the iron-rich phosphate glasses.

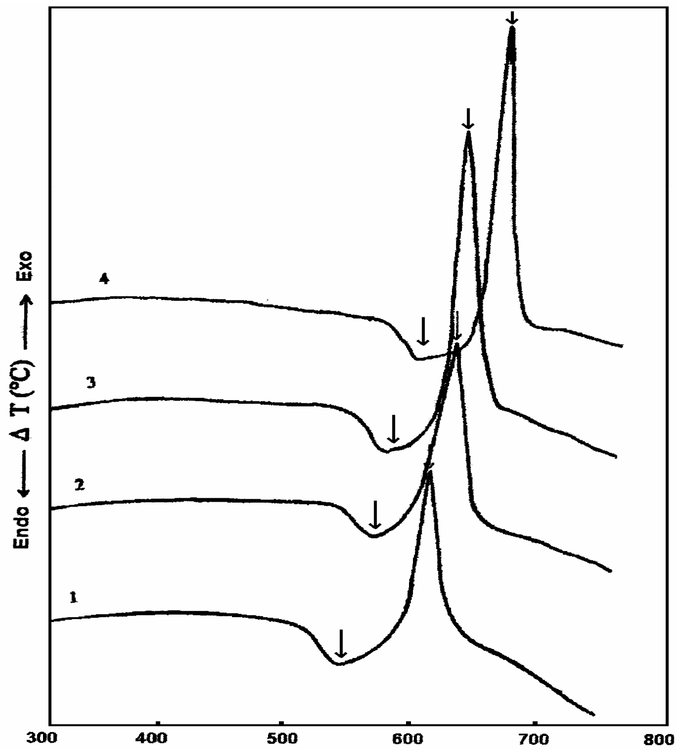

Fig.(4): Thermograms of (100- 2x) Fe_2O_3 – x PbO – x P_2O_5 glasses . Numbers in the figure represent glass numbers in table (1)

Table (1) : Characterization data for (Fe_2O_3 - PbO - P_2O_5) glasses

Glass No.	Composition (mol %)			I (arb. Units)	ΔH (Gauss)	Area ($x10^6$)	g factor	Density (g cm^{-3})	Δρ	Molar volume (cm^3mol^{-1})	Tg (°c)	Tc (°c)
	P_2O_5	PbO	Fe_2O_3									
1	60	20	20	173	125	2.703	2.0121 4.3489	4.375	0.179	41.289	550.79	624.81
2	65	17.5	17.5	189	122.5	2.836	2.0047	4.401	0.215	40.706	554.54	631.57
3	70	15	15	200	121.5	2.953	1.9974	4.429	0.247	40.077	559.68	638.49
4	75	12.5	12.5	340	100	3.400	2.0121	4.452	0.312	39.456	564.54	649.63

3.3. Infrared study:

Figure (5) shows the infrared spectra of the samples under study. All the measured spectra show the same six bands at 230, 360, 460, 540, 620 and 920-1080 cm^{-1}. Assignments of the observed bands are as follows:

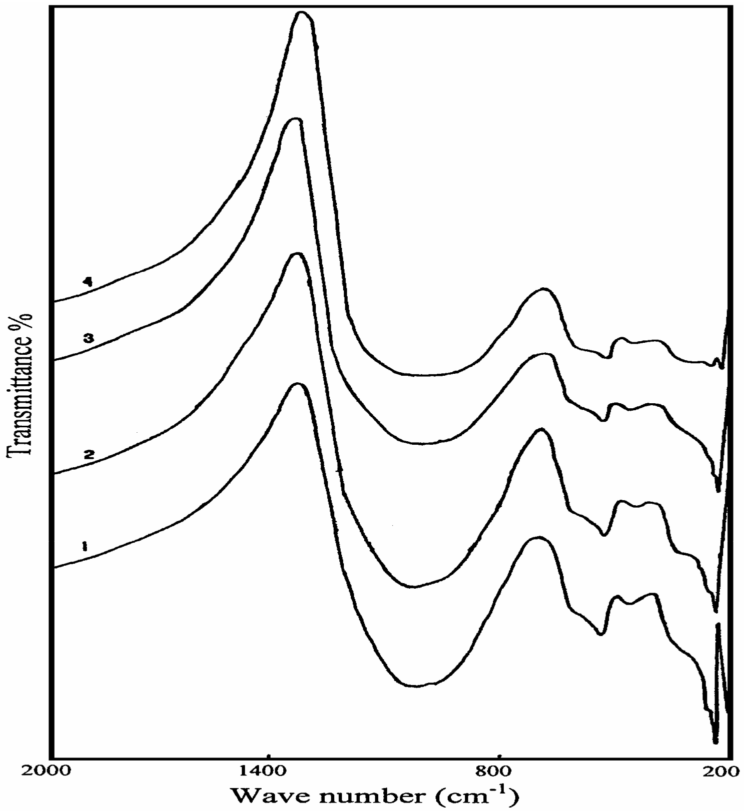

Fig.(5): Variation of area under the peak with iron content (mole %) in (100- 2x) Fe_2O_3 – x PbO – x P_2O_5 glasses. (Numbers represent glass numbers in Table (1)).

(i) Both the bands at 230 and 360 cm^{-1} are due to stretching vibrations of Fe-O group with different bond lengths. The existence of Fe^{3+} ions in octahedral structure was previously identified by the frequency bands appeared at 220, 365, 408, 460 and 610 cm^{-1} [29].

(ii) The band at 460 cm^{-1} observed in phosphate glasses was previously suggested to be due to FeO_6 and / or P_2O_7 groups [30].

(iii) The band in the range 920-1080 cm^{-1} was suggested to be due to metal-(PO_4)-link vibration [31, 32].

From the infrared spectra, it is noticeable that an increase in Fe_2O_3 concentration does not affect the position of any vibration peak The relative intensity I (460)/ I(1000) is detected to increase progressively with the increase of Fe_2O_3. This may reveal that on increasing Fe_2O_3 content the density of the Fe-O bonds increases on the expense of metal phosphate groups.

4. Conclusion:

1. An intense resonance peak at g ~ 2 is a characteristic feature of all the EPR spectra except that of the glass containing 60 mol % Fe_2O_3 which shows a weak band at g ~ 4.3.
2. The increasing value of the glass transition temperature with the Fe_2O_3 content indicates the increase of the degree of bridging, while the increased (T_c-T_g) value reflects the stability of these glasses.
3. It is noticeable that the presence of equimolar ratio of PbO and P_2O_5, within the range studied, not significantly affects the infrared spectra of iron-lead-phosphate glasses.

References:

1. B. Sreedhar, P. Indira, A.K. Bhatnagar and Kajuo Kojima, *J. Non-Cryst. Solids* **167,** 106 (1994).

2. B. Sreedhar, J. laxman Rao and S.V.J. laxman, *J. Non-Cryst. Solids* **116,** 111 (1990).

3. H. Toyuki and S. Akagi, *Phys. Shem. Glasses* **13**, 15 (1972).

4. Md. Shareefuddin, Md. Jamal, K. Vanaja, A. lyengar and M. Narsimha Chary, *J. Mater. Sci. lett*. **14**, 646 (1995).

5. Md. Shareefuddin, Md. Jamal and M. Nasimha Chary, *J. Non-Cryst. Solids* **201**, 95 (1996).

6. Md. Shareefuddin, Md. Jamal, G. Ramadenvudu, M. Laksipati Rao and M. Narasimha Chary, *J. Non-Cryst. Solids* **225**, 228 (1999).

7. B.C. Sales and L.A. Boater, *Science* **226**, 45 (1984).

8. P.Y. Shish, S.W. Yung and T.S. Chin, *J. Non-Cryst. Solids* **244**, 211 (1999).

9. C.M. Show and J.E. Shelby, *Phys. Chem. Glasses* **29**, 87(1988).
10. I.W. Donald, *J. Mater. Sci*. **28**, 2841 (1993).
11. C.M. Show and J.E. Shelby, *J. Am. Ceram. Soc*. **17**, C 252 (1998).
12. R.K. Brow, *J. Am. Ceram. Soc*. **76**, 913 (1993).
13. R.K. Brow, R.J. Kirkpatrick and G.L. Turner, *J. Am. Ceram. Soc*. **76**, 919 (1993)
14. Y. He. and D.E. Day, *Glass Technol*. **33**, 214 (1992).
15. H.S. Lin, P.Y. Shish and T.S. Chin, *Phys. Chem. Glasses* **37**, 227 (1996).
16. M.A. Tindyala and W.R. Ott, *Am. Ceram. Soc. Bull*. **57**, 432 (1978).
17. A.J. Bourdillon and F. Khumalo, *J. Bordas, Phil. Mag*. **B 37**, 731 (1978)
18. J. Robertson., *Phil. Mag*. **B 43**, 497 (1981).
19. M. lacovacci, E.C. Silva, H. Vargas and E.A. Pinheiro, *J. Appl. Phys*. **65**, 5150 (1989).
20. M.L. Baesso, E.C. Silva, F.C.G. Gandro and H. Vargas, *Phys. Chem. Glasses* **31**, 122 (1990).
21. T. Castner, G.S. Newell, W.C. Holton and C.P. Slichter, *J. Chem. Physics*. **32**, 668 (1980).
22. A.K. Band yo Padhyay, J. Zarjychi and P. Auric, *J. Non- Cryst. Solids* **40**, 353 (1980).
23. K. Tanaka, K Kamiya, T. Yoko, S. Tanabe and N. Soga, *Phys. Chem. Glasses* **32**, 16(1991).
24. D.W. Moon, J.M. Aitken, R.K. Macerone and G.G.Cielosjgk, *Phys. Chem. Glasses* **16**, 91 (1975).
25. N. Kishor, T.K. Bansel and R.G. Mendiratte, *Phys. Chem. Glasses* **25**, 52 (1984).
26. C.F. Drake, J.A. Stephens and B. Yates, *J. Non-Cryst. Solids* **28**, 61 (1978).
27. T. Nishida and T. Takashima, *Bull. Chem. Soc. Jap.* **60**, 941 (1987).
28. M. Samira Rabie and Hajjar Balkees, *Proc. Indian Acad. Sci*. **96**, 315 (1986).
29. A.M. Sanad, I. Kashif, A.A. El Sharkawy, A.A. El Sagheir and H. Farouk, *J. Mater. Sci*. **21**, 3483 (1986).
30. E.Z. Arlidge and V.C. Farmer. *J. Appl. Chem*. **13**, 17 (1963).
31. U. Selvaraj and K.J. Rao, *J. Non- Cryst. Solids* **104**, 300 (1988).